

A Novel Tunable Comblin Bandpass Filter Based on External Quality Factor and Internal Coupling Tunings

Lixue Zhou¹, Shijie Liu², Jun Duan¹, and Min Xun¹

¹Microwave Engineering of Department
Xi'an Electronic Engineering Research Institute, Xi'an 710100, P. R. China

²Microwave Engineering of Department
Shanghai Aerospace Electronic Technology Institute, Nanjing 201109, P. R. China
Vesslan_zhou@163.com, lsjjs@163.com, nwpuduan@163.com

Abstract — A comblin filter with quasi-elliptic performance with external quality factor and internal coupling tuning is presented in this paper. In this design, a wide center frequency tuning range with a constant 3-dB FBW (fractional bandwidth) and ABW (absolute bandwidth) is obtained. Also, it is demonstrated that the transmission zero located at the lower edge of passband can be adjusted with little effect on the passband characteristic. A prototype of the tunable filter with a tuning range of 1.27GHz to 2.25GHz is fabricated on a substrate with $\epsilon=10.2$ and $h=1.27$ mm. Through tuning internal coupling coefficient and external quality factor, one can make the filter operate over a wide center frequency tuning range, with a constant 3-dB FBW (fractional bandwidth) nearly kept at 54% or ABW (absolute bandwidth) nearly kept at 500 MHz.

Index Terms—Absolute bandwidth, coupling coefficient, fractional bandwidth, quality factor, tunable filter, transmission zero.

I. INTRODUCTION

Tunable bandpass filter is increasingly concerned in recent years, which is available to reduce the overall size and complexity of the modern communication and radar systems. Compared with other tunable filters, the comblin topology is most frequently applied in the circuit design, due to its several advantages, such as miniaturization, one unique transmission zero in the upper band, convenience for integration and so on [1-9]. In [1-2], the designed method on the basis of the detailed formulas for a fundamental comblin bandpass filter is presented, also its application is discussed. In [3-4], the resonator of SIR is utilized to keep the absolute bandwidth constant during the center frequency tuning. In [5], the short-circuited end of the resonator applied in comblin filter is replaced by the lumped series resonator. And a wide tuning range can be achieved with only a small capacitance ratio of varactor. In [6], two coupled

lines are introduced between the adjacent resonators to produce the source/load coupling and the multi resonator coupling. Then five tunable transmission zeros are created at the upper passband. In [7], the series RC unit is added to the first and last resonator to make the Q factor distribution of the resonator non-uniform. And then the passband flatness and selectivity of the filter are enhanced. In [8-9], the tunable filter with constant fractional bandwidth and absolute bandwidth is designed. Due to the cross coupling mechanism of the comblin filter, transmission zeroes is always produced only at the upper passband edge, thus improving the selectivity of the filter at one side. However, the smoothing decrease of the rejection at the lower passband limits its practical application. Thus, another new transmission zero should be created at the lower passband to tackle the problem.

Several tunable comblin filters with elliptic function performance have been designed [10-12]. In [10], a three-pole comblin filter with two tunable transmission zeros located at two edges of the passband is presented. The additional transmission zero at the lower side is created due to a section line shunted with a varactor. In [11], a cross coupling between the non-adjacent resonators is produced, thus a new transmission zero is supposed to be generated to give the filter a quasi-elliptic performance. It is noted that [12] firstly demonstrates a four-pole comblin filter with a pair of tunable transmission zeros at the two edges. And the phase difference between the main transmission path and other paths is analyzed to explain the production of the zeros. However, although some improvement is made to the performance of comblin filter, how to simultaneously adjust the external quality factor and the internal coupling coefficient to control the bandwidth and control the position of the novel transmission zero is not discussed.

In this paper, a novel comblin bandpass filter in Fig. 1 is presented. Varactors are employed to connect the adjacent resonators, the resonator and the I/O coupling

transmission line to tune the external quality factor and internal coupling tuning together. Therefore, the relative bandwidth and absolute bandwidth can be adjusted during the center frequency tuning, and in the paper *FBW* or *ABW* is nearly invariable in the process of the center frequency change. In addition, the application of a novel transmission line which produces the cross coupling between the I/O transmission lines creates a novel tunable transmission zero at the lower passband edge, thus, improving the selectivity of the designed filter. In this way, the tunable filter with fixed bandwidth can be used to connect with frequency synthesizer (PLL or DDS) which produces frequency-hopping signal of constant bandwidth to suppress spurious signal. And also, the filter is considered as a candidate for the switching-filter component which is frequently composed by several filters of adjacent passband. Detailed theoretical design, simulation, and experimental results for the tunable filter are demonstrated and discussed below.

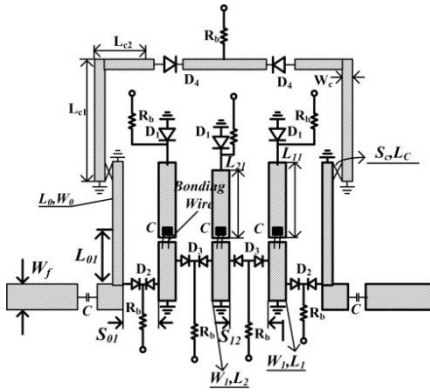


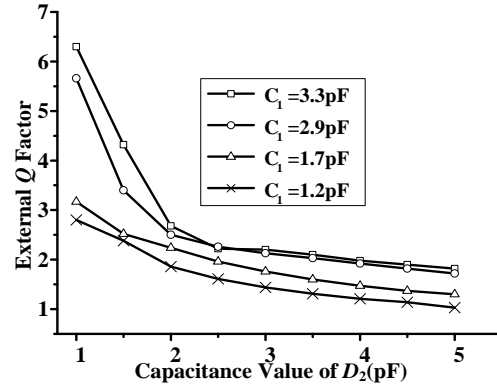
Fig. 1. Circuit of proposed tunable combline bandpass filter ($W_f=1.2\text{mm}$; $W_0=0.4\text{mm}$; $W_l=0.8\text{mm}$; $W_c=0.4\text{mm}$; $S_{0f}=0.3\text{mm}$; $S_{12}=0.2\text{mm}$; $S_c=0.2\text{mm}$; $L_{c1}=5.6\text{mm}$; $L_{c2}=1.5\text{mm}$; $L_c=2.8\text{mm}$; $L_l=6.8\text{mm}$; $L_2=6.4\text{mm}$; $L_{01}=1.45\text{mm}$).

II. ANALYSIS AND DESIGN OF THE PROPOSED TUNABLE FILTER

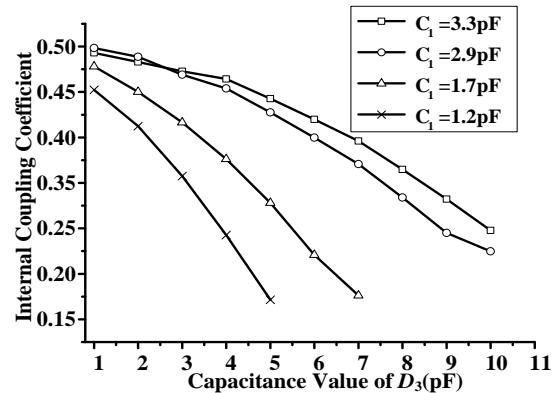
In Fig. 1, the circuit configuration of the proposed tunable filter is shown. It can be seen that thirteen varactors marked as D_1 , D_2 , D_3 , and D_4 are applied to satisfy the requirement for center frequency, internal coupling coefficient, external Q factor and the transmission zero tuning. Besides, to provide the *DC* power, several blocking capacitors C are utilized. What's more, a cross coupling path are introduced here to bring an additional transmission zero at lower passband. And, the characteristic impedances of the two microstrip lines at the input/output ports are both 50Ω .

It is clear from Fig. 1 that the varactor D_2 is applied to change the external Q factor of the filter, while D_3 used to tune the internal coupling coefficient. And

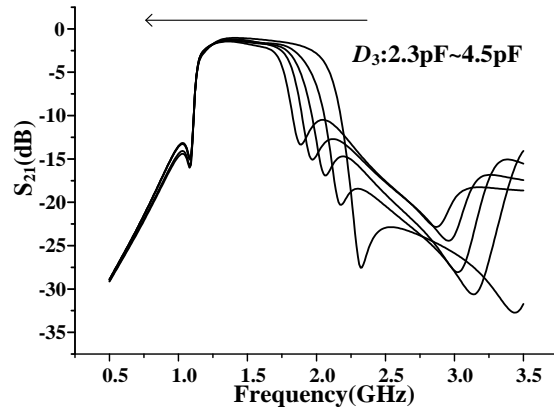
the technique to calculate the Q factor and coupling coefficient can be found in [13-14]. Hence, Fig. 2 (a) is drawn to present the relationship between the Q factor and capacitance value of D_2 , while the coupling coefficient vs. capacitance value of D_3 is given in Fig. 2 (b). In the figures, four capacitance values of D_1 that controls center frequency are considered. As is known, $Q=g_0g_1/FBW$ and $M_{i,i+1}=FBW/(g_i g_{i+1})$. Thus, various combination of Q and $M_{i,i+1}$ means different bandwidth. Taking $D_1=1.2\text{pF}$ as an example, 52.3% of *FBW* which is the final result in this paper will be obtained when making D_2 and D_3 equal 1.1pF and 1.3pF.



(a)



(b)



(c)

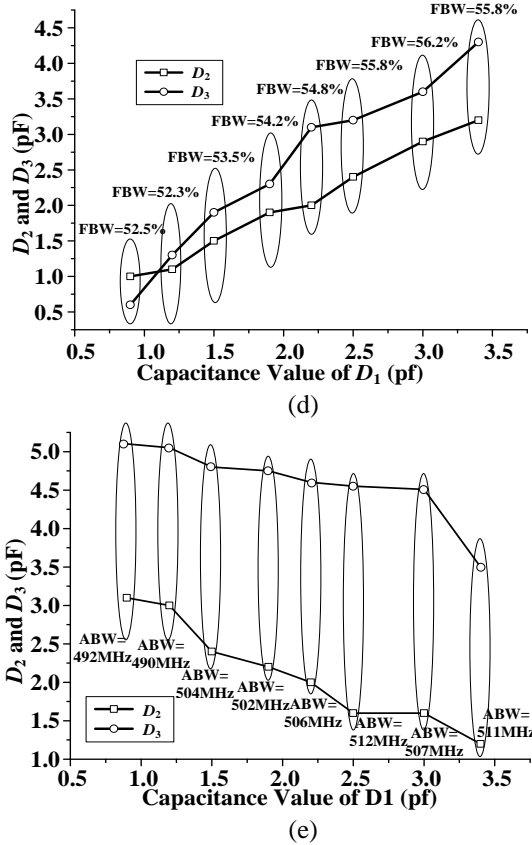


Fig. 2. (a) The relationship between external Q factor and capacitance value of D_2 ; (b) the relationship between internal coupling coefficient and capacitance value of D_3 ; (c) bandwidth change during the adjustment of D_2 and D_3 ; (d) the constant FBW during the center frequency moving; (e) the constant ABW during the center frequency moving.

To demonstrate the tunable characteristic for the bandwidth, Fig. 2 (c) which represents the variation process of bandwidth are plotted for the fixed value of D_1 (1.9pF) and D_4 (4.2pF). It is found that FBW is adjusted from 46.6% to 60.4% during the D_3 's decreasing. And it should be remembered that a wider tuning range of FBW will be gotten, if expanding value's limit of D_2 and D_3 . Figure 2 shows that the external Q factor and the internal coupling coefficient are inversely proportional to the capacitance value of D_2 and D_3 . And for a fixed value of D_2 and D_3 , the decrease of D_1 will lead to the decrease of Q factor and coupling coefficient [15-18]. Thus, to maintain the FBW as a constant, D_2 and D_3 should be adjusted simultaneously to keep the Q factor and coupling coefficient almost unchanged. Considering the element values $g_0=g_4=1$, $g_1=g_3=1.2275$ and $g_2=1.1525$ for Chebyshev lowpass prototype filters as an example, FBW of about 56% will be obtained when D_1 is made to be 3.4pF which tends to locate the center frequency of

filter around 1.26GHz, while D_2 and D_3 which respectively determine the external Q factor and internal coupling coefficient are equal to be 3.2pF and 4pF. D_4 deciding the position of novel transmission zero is assigned 7.1pF on the basis of the technique involved below. And from Fig. 2 (d), with the decrease of the value of D_1 , one should correspondingly reduce the values of D_2 and D_3 simultaneously to fix the FBW depending on Fig. 2 (a) and Fig. 2 (b). And, properly adjusting the values of D_2 and D_3 , FBW can be almost unchanged in the whole process of center frequency tuning. What's more, it is seen from Fig. 2 (e) that properly adjusting D_2 and D_3 simultaneously, the absolute bandwidth (ABW) can also be almost unchanged during the D_1 change. To maintain a constant ABW during the increase of center frequency, the coupling coefficient should be decreased and the external quality increased.

For the conventional combline tunable filter, one transmission zero is always created at the upper passband edge, thus improving the selectivity of the filter at one side. So, another transmission zero should be produced at the lower passband to improve the rejection. In this paper, an additional signal propagation path whose equivalent circuit model is shown in Fig. 3 (a) is introduced from input coupling line to the output one. Hence, the quasi-elliptic performance is expected because of the multiple path cancellation. And the location of novel transmission zero is decided by the resonating frequency of the coupled lines.

Figure 3 (b) and Fig. 3 (c) show the odd mode and the even mode equivalent circuit. It is obvious from Fig. 3 (c) that even mode resonating frequency is non-adjustable. In this case, the odd mode resonating frequency which can be controlled by D_4 is used to adjust the novel transmission zero. S_{11o} of the odd mode equivalent circuit in Fig. 3 (b) can be written as $S_{11o}=(Y_o-Y_{ino})/(Y_o+Y_{ino})$, where Y_o is the characteristic admittance of the circuit, $Y_{ino}=(-Y_{11}\times Y_{in}-Y_{11}^2-Y_{12}^2)/(-Y_{in}-Y_{11})$, where Y_{11} , Y_{in} and Y_{12} can be found as below:

$$Y_{11} = Y_{22} = -j0.5(Y_{oe} + Y_{oo}) \cot(\theta), \quad (1)$$

$$Y_{12} = Y_{21} = -j0.5(Y_{oe} - Y_{oo}) \csc(\theta), \quad (2)$$

$$Y_{in} = j \frac{(Y_4 \omega C + Y_4^2 \tan(\theta))}{(Y_4 - \omega C \tan(\theta))}. \quad (3)$$

In the equations, Y_{oe} and Y_{oo} denote the even mode characteristic impedance and the odd mode characteristic impedance of the coupling line, $\theta = \theta_e \neq \theta_o$. And the odd mode resonating frequency which makes $S_{11o}=0$ true, identifies the location of transmission zero. And, the equivalent circuit simulation in ADS (Advanced Design System) also indicates the resonating frequency of odd mode and even mode. In addition, Fig. 3 (d) is presented to demonstrate how the value of D_4 influences the resonating frequency.

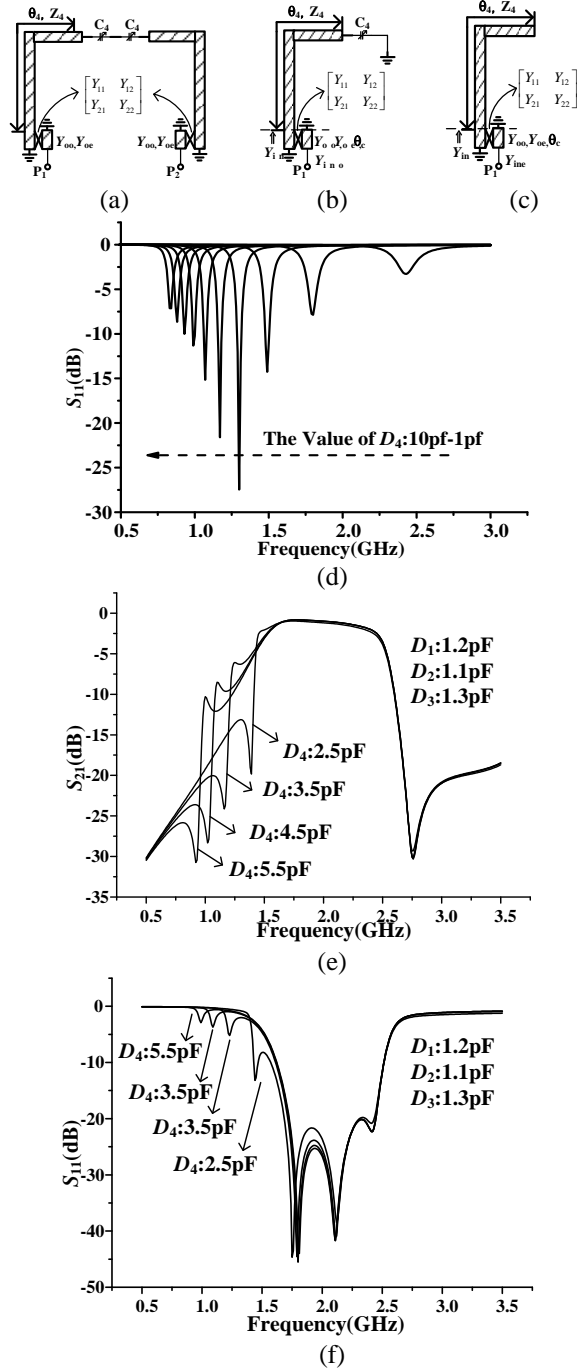


Fig. 3. (a) Equivalent circuit of the new transmission path; (b) the odd mode equivalent circuit; (c) the even mode equivalent circuit; (d) the odd mode resonating frequency of the added coupled line ($Z_4=75.6\Omega$; $\theta_4=8.7^\circ$; $Z_{oc}=107\Omega$; $Z_{oo}=37\Omega$; $\theta_c=8.7^\circ$ for $f_0=1\text{GHz}$); (e) S_{21} simulation result for $D_1=1.2\text{pF}$; (f) S_{11} simulation result for $D_1=1.2\text{pF}$.

In conclusion, the resonating frequency is inversely proportional to the value of D_4 . To further demonstrate

how the produced transmission zero is controlled by D_4 , Fig. 3 (e) and Fig. 3 (f) are given. And, the proper value should be set to D_2 and D_3 based on Fig. 2 (a) and Fig. 2 (b). What is shown in Fig. 3 has proven that adjustment of D_4 results in the change of the transmission zero at lower band. However, as the novel transmission zero moved away from the passband, a resonating transmission pole becomes increasingly obvious. Hence, to tackle the problem, the value of D_4 is chosen carefully to make the lower transmission zero approach passband.

III. DESIGN OF THE TUNABLE FILTER

Based on the analysis above, the design parameters are determined as follows:

Step 1): Select the third-order low-pass prototype with elements. Then calculate the external quality factors Q_e and the coupling coefficient M_{ij} through $Q=g_0g_1/FBW$ and $M_{i,i+1}=FBW/(g_i g_{i+1})$, where FBW is the 3-dB fractional bandwidth.

Step 2): Determine the dimensions of the proposed tunable resonator. Initially, the impedance of the transmission line is conveniently selected as 72Ω ($W_1=0.5\text{mm}$ is chosen initially), and the electrical length of the coupled line is set to 45 degrees at 1.7GHz ($L=7.4\text{mm}$), according to the required frequency tuning range. The spacing S_{12} between two resonators can then be determined. An initial value for S_{12} is chosen such that the coupling coefficient of the coupled resonators satisfies the bandwidth requirement at the center frequency.

Step 3): The rest of the design parameters are then determined. The coupling I/O structure is adopted to satisfy the constant bandwidth requirement over a wide tuning range because it has wideband matching behavior. The input/output line is typically chosen to be a high impedance line for tight coupling. S_{01} and W_0 are then chosen to satisfy external quality factors Q_e , using the well-known coupling coefficient/external Q_e method described in [13].

Step 4): An additional signal propagation path shown in Fig. 3 (a) is employed from input coupling line to the output one to create a novel transmission zero. And equivalent circuit technique is adopted to find the initial value of S_c and L_c . In the paper, short coupling lines of 15 degrees in length are chosen. And S_c is selected to be the same as S_{12} for simplicity.

Step 5): Finally, some necessary optimization is carried out, making use of electromagnetic EM simulation in SONNET. The estimated circuit dimensions from previous steps are substituted into a full wave EM simulator for including discontinuity, via-hole, and non-adjacent coupling effects. And when the center frequency is changed by D_1 , another group of value for D_2 , D_3 and D_4 units must be updated to keep the good passband performance based on Fig. 2 and Fig. 3.

A tunable filter of constant bandwidth is designed

on RT/Duroid 6010 with $\epsilon_r=10.2$ and $h=1.27\text{mm}$ with an overall size of $22\times 25\text{mm}^2$. Electro-magnetic simulation software of SONNET is applied for the optimization. Three kinds of silicon junction varactor diodes produced by Nanjing Electronic Devices Institute are applied. *WB62* ($C_i=0.45\sim 4.23\text{pF}$; $R_s=1\Omega$; $Q=3000$ at 50MHz for $C_i=1.07\text{pF}$) is selected as D_1 to accomplish the center frequency tuning, while the wide tuning range varactor *WB2011H* ($C_i=1.79\sim 20.53\text{pF}$; $R_s=0.5\Omega$; $Q=1200$ at 50MHz for $C_i=6.73\text{pF}$) is chosen to adjust the location of the transmission zero. Besides, for the trivial space between the two adjacent resonators, the bondable chip varactor *W205* ($C_i=0.8\sim 11.54\text{pF}$; $R_s=1.2\Omega$; $Q=800$ at 50MHz for $C_i=3.55\text{pF}$) is considered as the candidate for the coupling coefficient and external Q factor control, and the bonding wire is applied to finish the connection. Murata 0402 lumped components and 100pF chip capacitors are used for DC blocking and biasing.

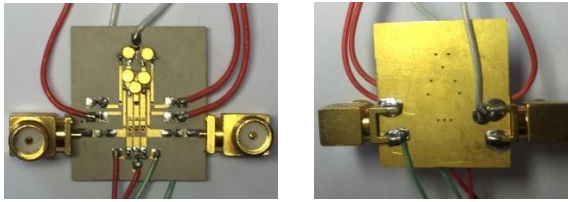


Fig. 4. Photography of the tunable combline filter.

In Fig. 4, the photography of the novel tunable filter is introduced. And the simulation and measured result in which the bandwidth is nearly kept unchanged are given in Fig. 5 and Fig. 6. The filter with the lowest center frequency 1.27GHz is optimized at the beginning ($D_1=3.4\text{pF}$, $D_2=3.2\text{pF}$, $D_3=4.3\text{pF}$, $D_4=7\text{pF}$). Then, D_1 is decreased to raise the center frequency to be 2.25GHz , while D_4 is reduced to move up the transmission zero correspondingly according to Fig. 3. Finally, D_2 and D_3 are adjusted monotonously to be 1pF and 0.6pF to keep a constant quality factor and coupling coefficient. Thus, nearly a constant fractional bandwidth can be acquired. And, for the case with unchanged absolute bandwidth during center frequency moving, D_2 and D_3 are tuned to be 1.2pF and 3.5pF .

According to [10], the following equation indicates that FBW and Q_u both mainly determine the insert loss of the filter:

$$IL(\text{dB}) = 4.343 \sum_{i=1}^n \frac{g_i}{\Delta Q_u}, \quad (4)$$

where Δ stands for the fractional bandwidth and Q_u represents the unloaded quality factor of resonator. Again, $g_0=g_4=1$, $g_1=g_3=1.2275$ and $g_2=1.1525$ for Chebyshev lowpass prototype filters are considered and Q_u of the resonator covers the value range of 50 to 90 during center frequency tuning. Thus, IL is almost less than 2dB for most tuning cases. However, the measured insertion

loss at the tuning range varies from 3dB to 5dB . This difference of IL is due to the *SMA* connector and the deviation of the diode's index.

Figure 5 and Fig. 6 demonstrate the simulated and measured results, with the center frequency turning from 1.27GHz to 2.25GHz . One can figure out that the filter achieves the quasi-elliptic performance. And the adjustment of D_4 makes the transmission zero close to the passband. Besides, D_2 and D_3 are changed correspondingly during center frequency tuning in order to keep the FBW and ABW invariant. As a result, the range of $52.5\%\sim 55.8\%$ of the fractional bandwidth and absolute bandwidth of $490\text{MHz}\sim 512\text{MHz}$ are obtained. To see the similarity, both the simulated and measured curves are plotted in one graph as shown in Fig. 5 and Fig. 6. Good agreement can be observed between the simulated and the experimental results. The slight frequency shift and difference of insert loss between measured and simulated results may be caused by the fabrication errors and the *SMA* connector. So, the comparing results given below have proven the advantage of the novel structure.

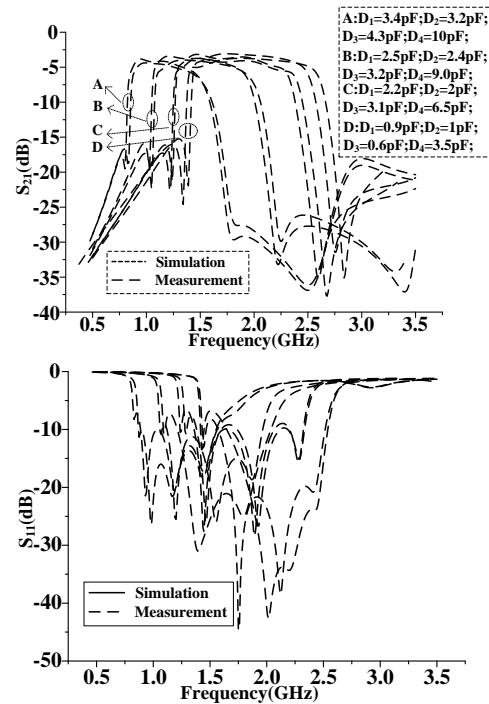


Fig. 5. Simulated and measured results of combline filter with constant FBW . (Voltage for the varactors during measurement is turning as below: $V_1:5.1\text{-}0.9\text{V}$; $V_2:11.3\text{-}1.9\text{V}$; $V_3:17.6\text{-}2.9\text{V}$; $V_4:19.4\text{-}3.1\text{V}$).

The comparisons of measured results for several tunable filters [5, 10-12] are shown in Table 1. It can be concluded that although the capacitance ratio for D_1 in this paper is not the smallest one, the tuning range of the

center frequency is wider than other compared structures. And as other tunable filters, the one introduced in the paper also have two transmission zeros at passband edges to improve the rejection. And the lower transmission zero can even be adjusted. Finally, being different from other tunable filters, *FBW* can almost be invariant during center frequency changing for the designed one in the paper.

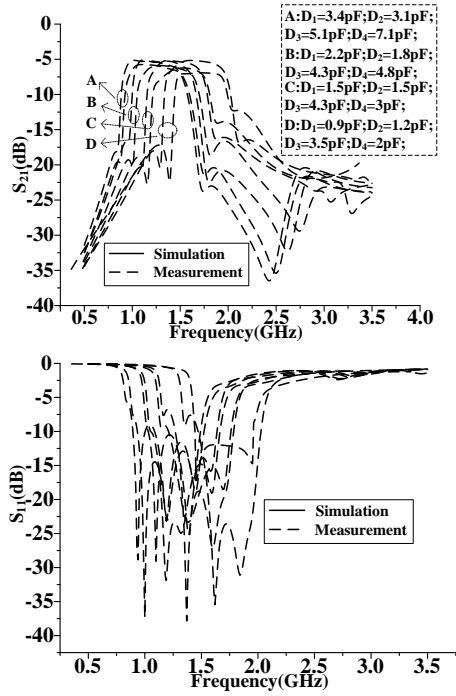


Fig. 6. Simulated and measured results of combline filter with constant ABW. (Voltage for the varactors during measurement is turning as below: $V_1:5.1\text{-}0.9\text{V}; V_2:11.7\text{-}2.1\text{V}; V_3:9.2\text{-}1.6\text{V}; V_4:19.4\text{-}3.1\text{V}$).

Table 1: Comparisons with wideband filters

| Ref. | Tuning Range (GHz) | C Ratio | Size (λ_{g0} @2GHz) | Diode Number | Elliptic |
|------|--------------------|---------|------------------------------|--------------|----------|
| [5] | 1.7~2.2 | 2.6 | 0.35×0.51 | 4 | No |
| [10] | 1.5~2.2 | 6.7 | 0.20×0.28 | 9 | Yes |
| [11] | 1.75~2.25 | 6.7 | 0.18×0.26 | 5 | Yes |
| [12] | 1.55~2.1 | 5.6 | 0.21×0.30 | 10 | Yes |
| This | 1.27~2.25 | 3.8 | 0.37×0.42 | 13 | Yes |

IV. CONCLUSION

In this work, a 1.27~2.25GHz tunable combline bandpass filter based on external quality factor and internal coupling tuning is proposed. During the tuning of the center frequency, coupling coefficient and external quality factor are adjusted to keep the bandwidth as a constant value. Additionally, a novel transmission line is applied to generate the coupling between the *I/O*

transmission lines to produce a new tunable transmission zero at the lower passband edge. Moreover, the quasi-elliptic performance can be observed at the simulation and measurement results. Therefore, the proposed filter exhibits good frequency selectivity, suggesting a good substitute for radio communication application.

REFERENCES

- [1] I. C. Huncter and J. D. Rhodes, "Electronically tunable microwave bandpass filters," *IEEE Trans. Microw. Theory Tech.*, vol. 30, no. 9, pp. 1353-1360, Sep. 1980.
- [2] P. W. Wong and I. Huncter, "Electronically tunable filters," *IEEE Microw. Mag.*, vol. 10, no. 6, pp. 46-54, Oct. 2009.
- [3] B. W. Kim and S. W. Yun, "Varactor-tuned combline bandpass filter using step-impedance microstrip lines," *IEEE Trans. Microw. Theory Tech.*, vol. 52, no. 4, pp. 1279-1283, Apr. 2004.
- [4] L. Zhang, X.-H. Wang, Z.-D. Wang, Y.-F. Bai, and X.-W. Shi, "Compact electronically tunable microstrip dual-band filter using stub-loaded SIRs," *J. Electromagn. Waves Appl.*, vol. 28, no. 1, pp. 39-48, Jan. 2004.
- [5] X. G. Wang, Y. H. W. Cho, and S. W. Yun, "A tunable combline bandpass filter loaded with series resonator," *IEEE Trans. Microw. Theory Tech.*, vol. 60, no. 6, pp. 1569-1576, June 2012.
- [6] S. R. Manuel, "High-selectivity tunable planar combline filter with source/load-multiresonator coupling," *IEEE Microw. Wireless Compon. Lett.*, vol. 17, no. 7, pp. 513-515, July 2007.
- [7] N. Jia, W. X. Tang, Z. C. Hao, and J. S. Hong, "An investigation of performance enhancement for tunable microstrip filter," in *2011 European Microw. Conf.*, pp. 472-475, Oct. 2011.
- [8] D.-H. Jia, Q.-Y. Feng, X.-G. Huang, and Q.-Y. Xiang, "A two-pole tunable filter with constant fractional-bandwidth characteristics," *Inter. J. Electro.*, vol. 101, no. 7, pp. 983-993, July 2014.
- [9] B. Liu, F. Wei, Q. Y. Wu, and X. W. Shi, "A tunable bandpass filter with constant absolute bandwidth," *J. Electromagn. Waves Appl.*, vol. 25, no. 11-12, pp. 1596-1604, Jan. 2011.
- [10] Y. C. Chiou and G. M. Rebeiz, "Tunable three-pole 1.5-2.2-GHz bandpass filter with bandwidth and transmission zero control," *IEEE Trans. Microw. Theory Tech.*, vol. 59, no. 11, pp. 2872-2878, Nov. 2011.
- [11] Y. C. Chiou and G. M. Rebeiz, "A quasi elliptic function 1.75-2.25 GHz 3-pole bandpass filter with bandwidth control," *IEEE Trans. Microw. Theory Tech.*, vol. 60, no. 2, pp. 244-249, Feb. 2012.
- [12] Y. C. Chiou and G. M. Rebeiz, "Tunable 1.55-2.1 GHz 4-pole elliptic bandpass filter with bandwidth control and > 50 dB rejection for wireless systems,"

IEEE Trans. Microw. Theory Tech., vol. 61, no. 1, pp. 117-124, Jan. 2013.

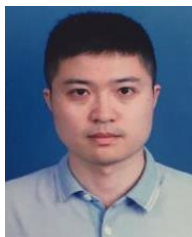
- [13] J.-S. Hong and M. J. Lancaster, *Microstrip Filters for RF/Microwave Applications*. New York: Wiley, 2001.
- [14] D. M. Pozar, *Microwave Engineering*. 2nd ed., New York: Wiley, 1998.
- [15] M. A. El-Tanani and G. M. Rebeiz, "Corrugated microstrip coupledlines for constant absolute bandwidth tunable filters," *IEEE Trans. Microw. Theory Tech.*, vol. 58, no. 4, pp. 956-963, Apr. 2010.
- [16] M. A. El-Tanani and G. M. Rebeiz, "High performance 1.5–2.5 GHz RF MEMS tunable filters for wireless applications," *IEEE Trans. Microw. Theory Tech.*, vol. 58, no. 6, pp. 1629-1637, June 2010.
- [17] Q. Xiang, Q. Feng, and X. Huang, "Tunable band-stop filter based on split ring resonators loaded coplanar waveguide," *Applied Computational Electromagnetics Society Journal*, vol. 28, no. 7, pp. 591-596, July 2013.
- [18] Y. Ma, W. Che, W. Feng, and J. Chen, "High selectivity dual-band bandpass filter with flexible passband frequencies and bandwidths," *Applied Computational Electromagnetics Society Journal*, vol. 28, no. 5, pp. 419-426, May 2013.



Lixue Zhou received the M.S. degree in Electromagnetic Fields and Microwave Technology from Nanjing University of Science and Technology, Nanjing, China, in 2010 and the Ph.D. degree in Electrical Engineering Department of Xidian University, Xi'an, China, in 2017.

Since 2010, he has been an Electronic Engineer in Xi'an Electronic Engineering Institute, where he developed the microwave and millimeter-wave circuit and RF component.

His research interests include microwave and millimeter-wave planar type circuit and multilayered circuit design and planner filter design in microwave and millimeter-wave frequency band.



Shijie Liu received the M.S. degree in Communication and Information Systems from Nanjing University of Science and Technology, Nanjing, China, in 2010. Since 2010, he has been an Electronic Engineer in Shanghai Aerospace Electronic Technology Institute, where he worked on microwave circuits and radar systems research.

His research interests include microwave circuit and frequency synthesizer.



Jun Duan received the M.S. degree in Electronics and Information Systems from Northwestern Polytechnical University, Xi'an, China, in 2011. Since 2011, he has been an Electronic Engineer in Xi'an Electronic Engineering Institute, where he worked on microwave circuits and radar systems research.

His research interests include multiband antennas, dual-polarized antennas, waveguide slot antenna arrays.



Min Xun received the M.S. degree in Electronics and Information Systems from Northwestern Polytechnical University, Xi'an, China, in 2002. Since 2002, he has been an Electronic Engineer in Xi'an Electronic Engineering Institute, where he worked on microwave circuits and receiver research.

His research interests include microwave and millimeter-wave planar type circuit and multilayered circuit design.